Dalton Transactions

Accepted Manuscript

ROYAL SOCIETY OF CHEMISTRY

www.rsc.org/dalton

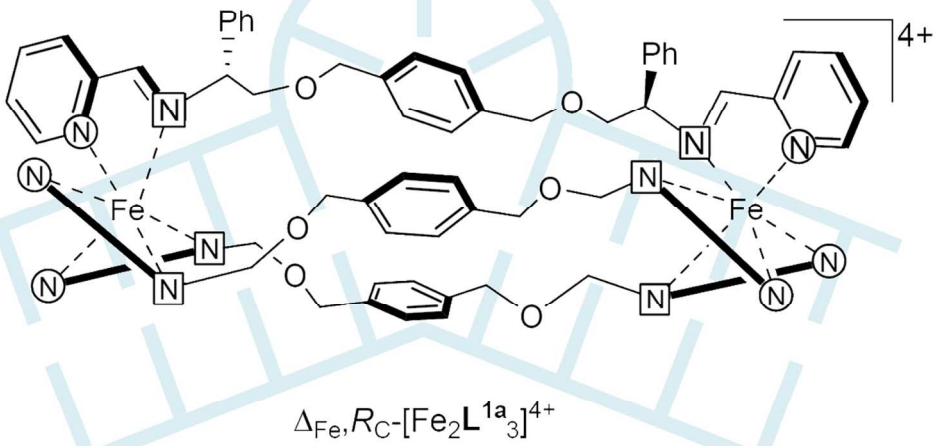

Δ_{Fe},R_C-[Fe_2**L**$^{1a}{}_3$]$^{4+}$

105x61mm (300 x 300 DPI)

Dalton Transactions

RSCPublishing

ARTICLE

Recognition of DNA/RNA bulges by antimicrobial and antitumor metallohelices

Cite this: DOI: 10.1039/x0xx00000x

Jaroslav Malina,[a] Peter Scott,[b] and Viktor Brabec*,[a]

Received 00th January 2015,
Accepted 00th January 2015

DOI: 10.1039/x0xx00000x

www.rsc.org/

Bulged structures have been identified in nucleic acids and have been shown to be linked to biomolecular processes involved in numerous diseases. Thus, chemical agents with affinity for bulged nucleic acids are of general biological significance. Herein, the mechanism of specific recognition and stabilization of bulged DNA and RNA by helical bimetallic species was established through detailed molecular biophysics and biochemistry assays. These agents, known as 'flexicates', are potential mimetics of α-helical peptides in cancer treatment, exhibiting antimicrobial and antitumor effects. The flexicates have positive impacts on the thermal stability of DNA duplexes containing bulges, which means that the flexicates interact with the duplexes containing bulges, and that these interactions stabilize the secondary structures of these duplexes. Notably, the stabilising effect of the flexicates increases with the size of the bulge, the maximal stabilization is observed for the duplexes containing a bulge composed of at least three bases. The flexicates bind most preferentially to the bulges composed of pyrimidines flanked on both sides also by pyrimidines. It is suggested that it is so because these bulges exhibit greatest conformational variability in comparison with other combinations of bases in the bulge loop and bases flanking the bulge. Finally, the results indicate that there is only one dominant binding site for the flexicates on the DNA and RNA bulges and that flexicates bind directly to the bulge or in its close proximity. It is also shown that the flexicates effectively bind to RNA duplexes containing the bulge region of HIV-1 TAR RNA.

Introduction

Bulged structures in nucleic acids are of general biological significance.[1] They have been proposed to play an important role in a number of biochemical processes, such as frame shift mutagenesis, RNA splicing, protein binding recognition, the ribosomal synthesizing machinery and expansion of triplet repeats during DNA synthesis.[2] Moreover, DNA repair proteins MutS[3] and RecA[4] bind preferentially to bulged structures, and also tumor suppression protein p53 prefers binding to bulges rather than other base mismatches in DNA.[5] Bulges have also been suggested as binding motifs for regulatory proteins involved with viral replication, including the TAR region of HIV-1.[6-8]

In view of the importance of bulges in biological systems, compounds capable of targeting bulged sequences could be used as valuable probes for studying their role in nucleic acids function or could even have significant therapeutic potential.[9] A number of attempts have been made to prepare such compounds. The most promising bulge binding agents discovered to date are: those based on NCS-chrom, a wedge-shaped enediyne antitumor antibiotic neocarzinostatin chromophore, 2-acylamino-1,8-naphthyridine, rhodium intercalators or the zinc(II) complex of 1-(4-quinoylyl)methyl-1,4,7,10-tetraazacyclododecane, and dinuclear ruthenium complexes.[10-15] Recently, we have demonstrated that DNA duplexes containing bulges are specifically recognized by $[Fe_2(\mathbf{I})_3]Cl_4$ ($\mathbf{I}$ = $C_{25}H_{20}N_4$) metallosupramolecular helicates (Fig. S1).[16] These molecules can also recognize other unusual DNA structures, such as Y-shaped three-way junctions,[17, 18] three-way junctions containing unpaired nucleotides, the so-called T-shaped three-way junctions[19] and human telomeric G-quadruplex DNA.[20] $[Fe_2(\mathbf{I})_3]Cl_4$ is synthesized as a mixture of two enantiomers (*M* and *P*, denoting left-handed and right-handed helical twist), which have different structural effects on DNA.[21, 22] Therefore, chromatographic resolution of the enantiomers is required.

A new strategy to prepare optically and diastereochemically pure monometallic complexes containing functionalized pyridine/imine units has been reported[23,24] including their use to create, *via* self-assembly process, water-stable, optically pure bimetallic structures with flexible linkers (Fig. 1A).[25,26] Since the stereoselectivity in these complexes does not rely on the helicate concept of mechanical coupling they are described as flexicates. The sense of chirality of the assembly is fully defined by the stereogenic centers in the organic part of the molecule. The discovery of the mechanism of steroechemical control in this type of complex was described[23] and then thoroughly investigated.[24] Each metal center has its stereochemistry completely (>99.5%) defined by a combination of steric effects and π-stacking interactions. Traditional helicates are different. They rely on mechanical coupling between metal centers (so-called helication). We do not notionally link our complex units together with various bridging groups that may be very flexible or

indeed actually work slightly against the intended stereochemistry at the metal (as in ligand $\mathbf{L^{1a}}$). While we have made some complexes that do in part exploit mechanical coupling[27] the examples in this manuscript do not. Thus, the term "helicate" is used in this article only for traditional ones. It has been shown that in addition to specific interactions with DNA, flexicates show promising antimicrobial activity towards methicillin-resistant *Staphylococcus Aureus* (MRSA) alongside modest toxicity towards the nematode worm *Caenorhabditis elegans*[26] and antitumor effects in particular in the tumor cells resistant to conventional cisplatin.[28]

We also showed in the precedent report[28] that $[Fe_2\mathbf{L^{1a}}_3]Cl_4$ flexicates (Fig. 1A) increase thermal stability of the DNA duplexes containing a one-, two- and three-adenine bulge. To explore binding of $[Fe_2\mathbf{L^{1a}}_3]Cl_4$ flexicates to DNA bulges further, we examined in the

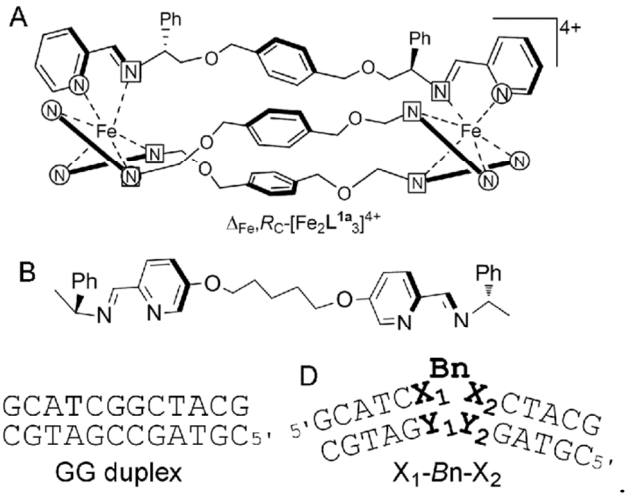

Fig. 1 A. Diastereomerically pure metallo-helical "flexicate" complexes of chiral ligands L^{1a}. Only one ligand shown in full. B. Chiral ligand L^{2a}. C: The fully complementary oligonucleotide duplex used as a control. D: Oligonucleotide duplexes containing a one-, two-, three-, four- and five-nucleotide bulge (*B* = A, T, G or C; n = 1-5) flanked by various combinations of bases X_1 and X_2. Y_1 and Y_2 correspond to complementary bases to X_1 and X_2, respectively.

present work the interactions of Λ- and Δ-enantiomers of $[Fe_2\mathbf{L^{1a}}_3]Cl_4$ with DNA duplexes containing bulges of various sizes and nucleotide sequences by means of biochemical and molecular biophysics methods. Moreover, the presence of structural motifs, such as bulges, may change the conformational flexibility of RNA molecules and the bulges themselves may just flip out exposing the internal regions of RNA to solvent and ligands. These factors play an important role in binding of different molecules to RNA.[29] Owing to the biological significance of RNA bulges we included in our study a three-nucleotide bulge embodied in TAR RNA that represents an attractive target for the intervention of human immunodeficiency virus type 1 (HIV-1) replication by small molecules.

Experimental

Chemicals

The iron(II) flexicates $[Fe_2\mathbf{L}^n_3]Cl_4$ were synthesised as previously described.[26] The synthetic oligodeoxyribonucleotides and oligoribonucleotides used in this work were purchased from VBC-genomics (Vienna, Austria). The quoted molar concentrations are related to the single strands. Stoichiometric amounts of oligonucleotides were mixed to form a duplex. Formation of double-stranded bulged structures was confirmed similarly as in our previous study[16] by electrophoresis in the native polyacrylamide gels. T4 polynucleotide kinase was purchased from New England Biolabs (Beverly, MA). [γ-^{32}P]-ATP was from MP Biomedicals, LLC (Irvine, CA). Acrylamide and bis(acrylamide) were from Merck KgaA (Darmstadt, Germany). Deoxyribonuclease I (DNaseI) was from Roche (Mannheim, Germany).

UV melting experiments

The stability of DNA bulges in the presence of the flexicates was monitored by measuring the absorbance at 260 nm (1 nm bandwidth, average time: 10 s, heating rate 0.4 °C/min) as a function of temperature. The experiment was run simultaneously on six masked 1 cm pathlength cuvettes of 1.2 mL volume using a Peltier controlled 6-sample cell-changer in a Varian Cary 4000 UV/vis spectrophotometer. Melting temperature (T_m) was calculated within the thermal heating program by applying a first derivative calculation. The concentration of oligodeoxyribonucleotides was $3x10^{-6}$ M per strand except 49 bp long duplexes that were measured at the concentration of $1x10^{-6}$ M per strand. The concentration of oligoribonucleotides was also $1x10^{-6}$ M per strand. The buffer conditions were sodium phosphate buffer (10 mM, pH 7.0) for oligoribonucleotides and sodium phosphate buffer (10 mM, pH 7.0) and 100 mM NaCl for oligodeoxyribonucleotides.

Gel electrophoresis of DNA/RNA bulges

One of the strands of oligodeoxyribonucleotide duplexes or TAR RNA were 5'-end labeled using T4 polynucleotide kinase and [γ-^{32}P]ATP. Stoichiometric amounts of oligodeoxyribonucleotides at the concentration of 1×10^{-5} M per strand were mixed together in the buffer to form a duplex. Flexicates were then added to the mixture at 25 °C so that the final concentration of the oligonucleotides in the samples was 5×10^{-6} M. The samples were analyzed by electrophoresis on 15% polyacrylamide gels in buffered solutions consisting of Tris(hydroxymethyl)amino methane (89 mM), borate (89 mM, pH 8.3) and EDTA (1 mM) run at 5 °C.

DNase I footprinting

Top or bottom strands of the oligonucleotide duplexes were 5'-end labeled using T4 polynucleotide kinase and [γ-^{32}P]ATP and hybridized with the complementary bottom or top strands. 5 μL solutions containing 1.11 × TKMC buffer (10 mM Tris pH 7.9, 10 mM KCl, 10 mM $MgCl_2$, and 5 mM $CaCl_2$), 3×10^{-4} M DNA (per nucleotide), and various concentrations of the flexicates were incubated for 15 min at 25 °C. Cleavage was initiated by the addition of 1 μL of DNase I diluted in the precedent experiment to the concentration that was sufficient to achieve partial cleavage of the DNA duplexes. Samples were allowed to react for 10 min at room temperature before quenching with 6 μL of 2× concentrated formamide loading buffer followed by incubation at 90 °C for 3 min. 2 μL of the mixture containing DNA cleavage products were then withdrawn and resolved by polyacrylamide (PAA) gel electrophoresis under denaturing conditions (8%/8 M urea PAA gel). The autoradiograms were visualized and quantified by using the bio-imaging analyzer.

Fluorescence spectroscopy

A solution of the oligonucleotide duplex (1 μM) was prepared in a 1 cm quartz cuvette in a total volume of 2.5 mL. The buffer was composed of sodium phosphate buffer (10 mM, pH 7.0) and NaCl (100 mM). Small volumes (2.5 μL) of flexicates were added to the solution to obtain the desired concentration and thoroughly mixed by pipetting. The mixture was kept undisturbed for 3 min at 25 °C. The fluorescence was measured by using Varian Cary Eclipse spectrofluorophotometer. The excitation and emission wavelengths were set to 310 nm and 365 nm, respectively, the excitation and emission slit widths were 5 nm, and the integration time was set to 5 s.

Other physical methods

UV absorbance measurements were conducted on a Varian Cary 4000 UV/VIS spectrophotometer equipped with a thermoelectrically controlled cell holder and quartz cells with the pathlength of 1 cm. The gels were visualized by using a BAS 2500 FUJIFILM bio-imaging analyzer and the radioactivity associated with the bands was quantified by using the AIDA image analyzer software (Raytest, Germany).

Results and discussion

DNA bulges

UV melting studies. We measured the DNA melting temperature (T_m) to compare binding affinities of the flexicates for DNA bulges of various sizes and nucleotide sequences. A series of typical melting curves for G-*C2*-G and C-*A2*-C DNA bulges in the presence of Λ- and Δ-$[Fe_2\mathbf{L^{1a}}_3]Cl_4$ are shown in the Figure S2 of the Supplementary Information. Importantly, under the conditions of the experiments of this study there is no measureable dissociation of the flexicates.[26] It is so because the metal-ligand complex is far away from notional equilibrium as the loss of ligand from the metal is effectively irreversible in water, so the crucial measurement is the kinetic stability. This is unusually high as a result in part of the presence of the hydrophobic π-stacking. Full kinetic analysis of this hydrolysis has been reported in our previous study,[26] which to our knowledge has not been reported for any other class of water-soluble helicate. Circular dichroic spectra of solutions of these flexicates in water showed no change over lengthy storage periods even in the presence of nucleic acids with no indications of stereochemical leakage. We also know from DNA titrations that the structure is completely retained on binding to the major groove. In order to effect dissociation we studied the stability at pH 1.5; even then the flexicate complexes of chiral ligands L1a showed only ca. 8% decomposition over 10 days. The T_m corresponds to the midpoint of a smooth transition obtained by recording the absorbance at 260 nm as a function of the temperature (Fig. S2). The changed T_m values of the duplexes [T_m of the duplex modified by the flexicate minus T_m of the control (unmodified duplex) (ΔT_m)] are generally affected by the oligonucleotides' dissociation constants and the stability of their own secondary structures. The stronger the interaction between DNA and $[Fe_2\mathbf{L^{1a}}_3]Cl_4$, the more the T_m value increases.[30,31]

Effect of the bulge size. The thermal stabilities of the oligonucleotide duplexes containing a four- and five-adenine bulge (B = A, n = 4, 5; Fig. 1D) in the presence of the flexicates were analysed and compared with the data for the duplexes containing a one-, two- and three-adenine bulge reported in our precedent study (Table 1).[28] The fully matched duplex of sequence identical to that of the bulged duplexes (Fig. 1C) was used as a control. Both 5'- and 3'-sides of the bulges were flanked by G·C pairs (X_1 = G, Y_1 = C, X_2 = G, Y_2 = C; Fig. 1D). The T_m values of the nonmodified duplexes in the absence of the flexicates decreased with increasing number of unpaired adenines in the bulge (Table 1) from 45.0 °C for G-*A1*-G to 38.7 °C and 35.2 °C for G-*A2*-G and G-*A3*-G, respectively, to 35.1 °C and 32.6 °C for G-*A4*-G and G-*A5*-G, respectively. The same duplex without a bulge had a melting temperature 54.9 °C. The results listed in Table 1 show that Λ- and Δ-$[Fe_2\mathbf{L^{1a}}_3]Cl_4$ have positive impacts on the thermal stability of DNA duplexes containing bulges and that the stabilising effect of the flexicates increases with the size of the bulge. Interestingly, the maximal stabilization of duplexes containing DNA bulges by Λ- and Δ-$[Fe_2\mathbf{L^{1a}}_3]Cl_4$ was observed for the duplexes containing a bulge of at least three bases (adenines). A further increase in the bulge size resulted in only a small enhancement of the stabilization of the bulged duplexes by the flexicates. The melting temperature of the duplexes was only slightly increased (1-2 °C) when the flexicate:bulge ratio was increased from 1:1 to 2:1 which is consistent with a single dominant binding site for the flexicates on these bulges. The only exception is the G-*A1*-G bulge whose T_m is moderately increased at 1:1 flexicate:bulge ratio, however on increasing the ratio to 2:1 the ΔT_m approximately doubles, suggesting the presence of at least two binding sites per duplex. The Λ-enantiomer was more efficient in stabilizing DNA bulges than the Δ-enantiomer, except for G-*A3*-G, where the Δ-enantiomer had slightly greater stabilizing effect.

Table 1 Thermal stability of a fully matched GG duplex and corresponding duplexes containing a one-, two-, three-, four- and five-adenine bulge in the presence of Λ- and Δ-$[Fe_2\mathbf{L^{1a}}_3]Cl_4$.

Compound	ΔT_m (°C) at 1:1[a]	ΔT_m (°C) at 2:1[b]
GG duplex (T_m = 54.9 °C)[c]		
Λ-$[Fe_2\mathbf{L^{1a}}_3]Cl_4$	1.2[c]	2.4[c]
Δ-$[Fe_2\mathbf{L^{1a}}_3]Cl_4$	0[c]	0[c]
G-*A1*-G (T_m = 45.0 °C)[c]		
Λ-$[Fe_2\mathbf{L^{1a}}_3]Cl_4$	3.6[c]	6.9[c]
Δ-$[Fe_2\mathbf{L^{1a}}_3]Cl_4$	1.4[c]	2.5[c]
G-*A2*-G (T_m = 38.7 °C)[c]		
Λ-$[Fe_2\mathbf{L^{1a}}_3]Cl_4$	4.6[c]	5.5[c]
Δ-$[Fe_2\mathbf{L^{1a}}_3]Cl_4$	4.2[c]	5.5[c]
G-*A3*-G (T_m = 35.2 °C)[c]		
Λ-$[Fe_2\mathbf{L^{1a}}_3]Cl_4$	8.2[c]	10.2[c]
Δ-$[Fe_2\mathbf{L^{1a}}_3]Cl_4$	8.8[c]	10.3[c]
G-*A4*-G (T_m = 35.1 °C)		
Λ-$[Fe_2\mathbf{L^{1a}}_3]Cl_4$	10.3	11.1
Δ-$[Fe_2\mathbf{L^{1a}}_3]Cl_4$	8.5	10.0
G-*A5*-G (T_m = 32.6 °C)		
Λ-$[Fe_2\mathbf{L^{1a}}_3]Cl_4$	11.2	12.6
Δ-$[Fe_2\mathbf{L^{1a}}_3]Cl_4$	8.2	9.7

[a]Flexicate:duplex was 1:1. [b]Flexicate:duplex was 2:1. [c]Data previously reported.[28]

In summary, the results demonstrating the effect of the bulge size examined by measuring the T_m (Table 1) suggest that in particular bulges of three or more bases (adenines) show some unique structural feature(s) not found in the fully matched duplex that are responsible for the enhanced affinity of Λ- and Δ-$[Fe_2\mathbf{L^{1a}}_3]Cl_4$ flexicates for these DNA bulges. The observation that the flexicates bind to a small bulge, composed of only one unpaired base, suggests that bulky flexicates based on the the $\mathbf{L^{1a}}$ ligand can stick to the bulge from its exterior. On the other hand, it cannot be

excluded that in the case of interaction of the flexicates with DNA bulges containing three bases or more, the bulge could create a cavity or pocket of the sufficient size capable to accommodate the bulkier flexicate molecule.

Effect of bases in the bulge loop and bases flanking the bulge. The effect of the composition of the bulge loop on the binding of Λ- and Δ-$[Fe_2\mathbf{L^{1a}}_3]Cl_4$ was also investigated. The melting of three oligonucleotide duplexes containing two unpaired thymines, cytosines and guanines (*B* = T, C, G, n = 2; Fig. 1D) and three duplexes containing three unpaired thymines, cytosines and guanines (*B* = T, C, G, n = 3; Fig. 1D) in the presence of the flexicates was recorded. Both 5'- and 3'-sides of the bulges were flanked by G·C pairs (X_1 = G, Y_1 = C, X_2 = G, Y_2 = C; Fig. 1D). Different compositions of the bulge loops affected differently the thermal stabilities of the duplexes (Tables 1 and 2). The melting temperatures of two-nucleotide bulges G-*T2*-G, G-*C2*-G and G-*G2*-G were 36.1 ˚C, 36.0 ˚C and 41.2 ˚C, respectively, while the melting temperatures of three-nucleotide bulges G-*T3*-G, G-*C3*-G and G-*G3*-G were 33.6 ˚C, 30.4 ˚C and 37.3 ˚C, respectively. As it can be seen in Tables 1 and 2, the presence of Λ- and Δ-$[Fe_2\mathbf{L^{1a}}_3]Cl_4$ stabilized DNA bulges containing loops composed of purines (G-*A2*-G, G-*G2*-G, G-*A3*-G and G-*G3*-G) less than bulges containing loops composed of pyrimidines (G-*T2*-G, G-*C2*-G, G-*T3*-G and G-*C3*-G). The greater stabilization of DNA bulges containing loops composed of pyrimidines was observed also for $[Fe_2\mathbf{(I)}_3]Cl_4$.[16] The Λ-enantiomer was more efficient in stabilizing DNA bulges than the Δ-enantiomer, except for G-*T3*-G, where the stabilizing effect of both enantiomers was identical.

The conformation of the bulges, and thus their interactions with the flexicates, might be expected to be affected by the types of bases flanking the bulge. We explored the effects of bases flanking the two- and three-adenine bulges on the binding affinities of Λ- and Δ-$[Fe_2\mathbf{L^{1a}}_3]Cl_4$. We used oligonucleotide duplexes containing a two- and three-adenine bulge (*B* = A, n = 2, 3; Fig. 1D) and various combinations of bases flanking the bulge (X_1 = C, T, A, T, A; X_2 = C, T, A, A, T; Y_1 = G, A, T, A, T; Y_2 = G, A, T, T, A for the two-adenine bulge and $X_1 = X_2$ = C, T, A; $Y_1 = Y_2$ = G, A, T for the three-adenine bulge; Fig. 1D). Variations of bases flanking the two-adenine bulge affected the melting temperatures of the duplexes in the following way: melting temperatures for C-*A2*-C, T-*A2*-T, A-*A2*-A, T-*A2*-A and A-*A2*-T were 36.8 ˚C, 25.7 ˚C, 33.8 ˚C, 31.2 ˚C and 32.8 ˚C, respectively. Variations of bases flanking the three-adenine bulge affected the melting temperatures of the duplexes in the following way: melting temperatures for C-*A3*-C, T-*A3*-T and A-*A3*-A were 33.2 ˚C, 23.0 ˚C and 30.4 ˚C, respectively. Results summarized in Tables 1 and 3 show that the thermal stability of DNA duplexes containing two or three unpaired adenines in the presence of the flexicates was higher if the bases flanking both the 5'-side and 3'-side of the bulge contained pyrimidines (C-*A2*-C, T-*A2*-T, C-*A3*-C and T-*A3*-T) rather than purines (G-*A2*-G, A-*A2*-A, G-*A3*-G and A-*A3*-A). Combinations of purine and pyrimidine as bases flanking the two-adenine bulge, as in the T-*A2*-A (pyrimidine-purine) or A-*A2*-T (purine-pyrimidine), gave lower enhancement of the thermal stability in the presence of the flexicates than if the purines flanked both sides of the bulge as in the case of A-*A2*-A. In all cases, the Λ-enantiomer increased thermal stability of DNA duplexes containing bulges more than the Δ-enantiomer.

Inspired by the results that we obtained in the previous experiments (Tables 1-3), we decided to explore the effect of the flexicates on the DNA bulges containing loops composed of pyrimidines (thymine) and flanked on both the 5'-side and 3'-side of the bulge by pyrimidines (cytosine) (*B* = T, n = 2, 3; $X_1 = X_2$ = C,

Table 2 Thermal stability of duplexes containing a two- and three-thymine, two- and three-cytosine and two- and three-guanine bulge in the presence of Λ- and Δ-$[Fe_2\mathbf{L^{1a}}_3]Cl_4$.

Compound	ΔT_m (˚C) at 1:1[a]	ΔT_m (˚C) at 2:1[b]
G-*T2*-G (T_m = 36.1 ˚C)		
Λ-$[Fe_2\mathbf{L^{1a}}_3]Cl_4$	14.0	14.9
Δ-$[Fe_2\mathbf{L^{1a}}_3]Cl_4$	12.6	13.4
G-*C2*-G (T_m = 36.0 ˚C)		
Λ-$[Fe_2\mathbf{L^{1a}}_3]Cl_4$	14.4	15.2
Δ-$[Fe_2\mathbf{L^{1a}}_3]Cl_4$	12.3	13.2
G-*G2*-G (T_m = 41.2 ˚C)		
Λ-$[Fe_2\mathbf{L^{1a}}_3]Cl_4$	7.8	10.1
Δ-$[Fe_2\mathbf{L^{1a}}_3]Cl_4$	4.3	7.0
G-*T3*-G (T_m = 33.6 ˚C)		
Λ-$[Fe_2\mathbf{L^{1a}}_3]Cl_4$	16.7	17.6
Δ-$[Fe_2\mathbf{L^{1a}}_3]Cl_4$	16.7	17.7
G-*C3*-G (T_m = 30.4 ˚C)		
Λ-$[Fe_2\mathbf{L^{1a}}_3]Cl_4$	18.2	18.8
Δ-$[Fe_2\mathbf{L^{1a}}_3]Cl_4$	16.7	18.1
G-*G3*-G (T_m = 37.3 ˚C)		
Λ-$[Fe_2\mathbf{L^{1a}}_3]Cl_4$	14.0	16.7
Δ-$[Fe_2\mathbf{L^{1a}}_3]Cl_4$	9.1	11.9

[a] Flexicate:duplex was 1:1. [b] Flexicate:duplex was 2:1.

Table 3 Thermal stability of duplexes containing a two- and three-adenine bulge with various combinations of bases flanking the 5'-side and 3'-side of the bulge in the presence of Λ- and Δ-$[Fe_2\mathbf{L^{1a}}_3]Cl_4$.

Compound	ΔT_m (˚C) at 1:1[a]	ΔT_m (˚C) at 2:1[b]
C-*A2*-C (T_m = 36.8 ˚C)		
Λ-$[Fe_2\mathbf{L^{1a}}_3]Cl_4$	9.3	10.3
Δ-$[Fe_2\mathbf{L^{1a}}_3]Cl_4$	6.3	7.7
T-*A2*-T (T_m = 25.7 ˚C)		
Λ-$[Fe_2\mathbf{L^{1a}}_3]Cl_4$	10.8	12.3
Δ-$[Fe_2\mathbf{L^{1a}}_3]Cl_4$	8.1	9.3
A-*A2*-A (T_m = 33.8 ˚C)		
Λ-$[Fe_2\mathbf{L^{1a}}_3]Cl_4$	8.1	9.9
Δ-$[Fe_2\mathbf{L^{1a}}_3]Cl_4$	6.7	8.5
T-*A2*-A (T_m = 31.2 ˚C)		
Λ-$[Fe_2\mathbf{L^{1a}}_3]Cl_4$	7.1	8.8
Δ-$[Fe_2\mathbf{L^{1a}}_3]Cl_4$	6.0	7.3
A-*A2*-T (T_m = 32.8 ˚C)		
Λ-$[Fe_2\mathbf{L^{1a}}_3]Cl_4$	6.1	9.7
Δ-$[Fe_2\mathbf{L^{1a}}_3]Cl_4$	4.8	6.2
C-*A3*-C (T_m = 33.2 ˚C)		
Λ-$[Fe_2\mathbf{L^{1a}}_3]Cl_4$	13.8	14.8
Δ-$[Fe_2\mathbf{L^{1a}}_3]Cl_4$	10.3	12.0
T-*A3*-T (T_m = 23.0 ˚C)		
Λ-$[Fe_2\mathbf{L^{1a}}_3]Cl_4$	13.6	15.3
Δ-$[Fe_2\mathbf{L^{1a}}_3]Cl_4$	10.2	11.8
A-*A3*-A (T_m = 30.4 ˚C)		
Λ-$[Fe_2\mathbf{L^{1a}}_3]Cl_4$	11.7	12.8
Δ-$[Fe_2\mathbf{L^{1a}}_3]Cl_4$	8.6	9.8

[a] Flexicate:duplex was 1:1. [b] Flexicate:duplex was 2:1.

$Y_1 = Y_2$ = G; Fig. 1D). Indeed, results listed in Table 4 confirm that the combination of the bulge loop composed of pyrimidines with pyrimidines as bases flanking the bulge, as in C-*T2*-C and C-*T3*-C, gave the highest increase of the T_m of DNA duplexes containing a two- or three-nucleotide bulge in the presence of the flexicates. In aggregate, these results indicate that the flexicates bind most preferentially to the bulges composed of pyrimidines flanked on both sides also by pyrimidines. This might be a consequence of the fact that extra pyrimidines in the bulges flanked by pyrimidines exhibit greatest conformational variability in comparison with other combinations of bases in the bulge loop and bases flanking the bulge.[32, 33]

Electrophoretic mobility shift assay. Similarly to our previous report[16] we used an electrophoretic mobility shift assay to explore whether the stability of the flexicate-DNA bulge complex is sufficient to withstand migration through a polyacrylamide gel. In these experiments we used 14 bp long duplexes with the central sequence which was identical with the sequence of the 12 bp duplexes used for the melting experiments (Fig. 1D). These duplexes were designed by the addition of the C·G pair on both ends of these 12 bp duplexes (see Fig. 3B as an example of the 14 bp duplex). The autoradiogram of the gel run at 5 ˚C (Fig. 2) shows interactions of the C-*T3*-C(14) bulge with Λ- and Δ-$[Fe_2\mathbf{L^{1a}}_3]Cl_4$. It can be seen that in the presence of the Λ- and Δ-enantiomer of $[Fe_2\mathbf{L^{1a}}_3]Cl_4$ (Fig. 2, lanes 1-8) there appears a new slower-migrating band indicating formation of a flexicate-DNA bulge complex. The intensity of the slower-migrating band increased with increasing flexicate:duplex ratio. The experiment was repeated under the same conditions with a number of other 14 bp long duplexes containing a two- or three-nucleotide DNA bulge. However, inspection of the gels (Fig. S3) never revealed formation of a flexicate-DNA bulge complex in the presence of Λ- and Δ-$[Fe_2\mathbf{L^{1a}}_3]Cl_4$ as for the C-*T3*-C(14) bulge. On the other hand, it is consistent with the results of the melting experiments (Table 4) demonstrating that the highest increase of the T_m values in the presence of Λ- and Δ-$[Fe_2\mathbf{L^{1a}}_3]Cl_4$ was observed for the C-*T3*-C bulge. In other words, the stability of other flexicate-DNA bulge complexes was not sufficient to withstand migration through a gel. Inspection of the gel in Fig. 2 also shows that the complex with the Λ-enantiomer was more stable in the gel than that with the Δ-enantiomer which is again in agreement with UV melting experiments (Table 4).

Table 4 Thermal stability of duplexes containing a two-thymine, two-guanine and three-thymine bulge flanked by C·G pairs on both sides in the presence of Λ- and Δ-$[Fe_2\mathbf{L^{1a}}_3]Cl_4$.

Compound	ΔT_m (˚C) at 1:1[a]	ΔT_m (˚C) at 2:1[b]
C-*T2*-C (T_m = 35.1 ˚C)		
Λ-$[Fe_2\mathbf{L^{1a}}_3]Cl_4$	16.2	17.1
Δ-$[Fe_2\mathbf{L^{1a}}_3]Cl_4$	11.1	12.4
C-*G2*-C (T_m = 34.1 ˚C)		
Λ-$[Fe_2\mathbf{L^{1a}}_3]Cl_4$	13.0	13.3
Δ-$[Fe_2\mathbf{L^{1a}}_3]Cl_4$	8.3	9.9
C-*T3*-C (T_m = 31.0 ˚C)		
Λ-$[Fe_2\mathbf{L^{1a}}_3]Cl_4$	18.5	19.4
Δ-$[Fe_2\mathbf{L^{1a}}_3]Cl_4$	16.6	18.2

[a] Flexicate:duplex was 1:1. [b] Flexicate:duplex was 2:1.

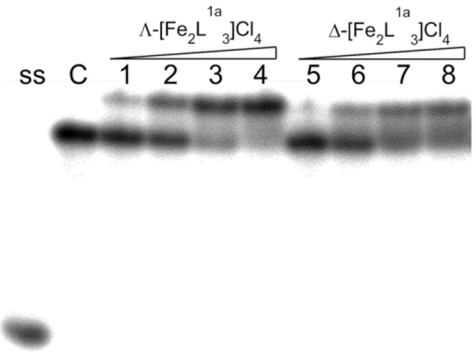

Fig. 2 Autoradiogram of the gel run at 5 ˚C, demonstrating interactions of the Λ- and Δ-$[Fe_2\mathbf{L^{1a}}_3]Cl_4$ with the C-*T3*-C(14) bulge. Lane ss: control containing one strand in the buffer. Lane C: control containing duplex in the buffer in the absence of the flexicates. Lanes 1-4: duplex mixed with Λ-$[Fe_2\mathbf{L^{1a}}_3]Cl_4$ at 0.5:1, 1:1, 1.5:1 and 2:1 (flexicate:duplex) ratios, respectively. Lanes 5-8: duplex mixed with Δ-$[Fe_2\mathbf{L^{1a}}_3]Cl_4$ at 0.5:1, 1:1, 1.5:1 and 2:1 (flexicate:duplex) ratios, respectively.

DNase I footprinting. In order to further characterize the binding of the flexicates to the DNA bulges, the Λ- and Δ-$[Fe_2\mathbf{L^{1a}}_3]Cl_4$ were mixed with the T-*A2*-T(14) and G-*C3*-C(49) (see Fig. S4 for its nucleotide sequence) duplexes at 0.25:1, 0.5:1, 0.75:1 and 1:1 flexicate:duplex ratios, respectively, and then partial cleavage by DNase I was performed (Figs. 3 and 4). The autoradiograms of the DNA cleavage-inhibition patterns for the T-*A2*-T(14) are shown in Fig. 3.

In the presence of both enantiomers cutting is markedly reduced in 5'-AAT sequence in the top strand corresponding to the two unpaired adenines and thymine flanking the bulge on the 3'-side (Fig. 3, left panel). In the bottom strand the presence of the flexicates inhibits the DNase I cleavage activity at the adenine residue paired with thymine flanking the 5'-side of the bulge and at the guanine residue separated by four base pairs from the bulge on the 5'-side. The sequence of the T-*A2*-T(14) bulge and sites protected by Λ- and Δ-$[Fe_2\mathbf{L^{1a}}_3]Cl_4$ from the cleavage by DNase I are summarized in Fig. 3B. The autoradiograms of the DNA cleavage-inhibition patterns for the G-*C3*-C(49) bulge are shown in Fig. 4. In this case, the presence of Λ- and Δ-$[Fe_2\mathbf{L^{1a}}_3]Cl_4$ reduced the DNase I activity in the 5'-GC sequence in the top strand corresponding to the guanine flanking the 5'-side of the bulge and the first cytosine of the loop. The DNase I activity in the bottom strand was moderately inhibited only by the Λ-$[Fe_2\mathbf{L^{1a}}_3]Cl_4$ in 5'-TGC sequence located directly opposite the bulge.

The results of the DNase I footprinting summarized in Figs. 3B and 4B are consistent with preferential binding of Λ- and Δ-$[Fe_2\mathbf{L^{1a}}_3]Cl_4$ to DNA bulges or in their close proximity. In addition, the results shown in Fig. 4 confirm that the flexicates also bind to a bulge containing DNA duplex that is markedly longer (49 bp) than 12 bp.

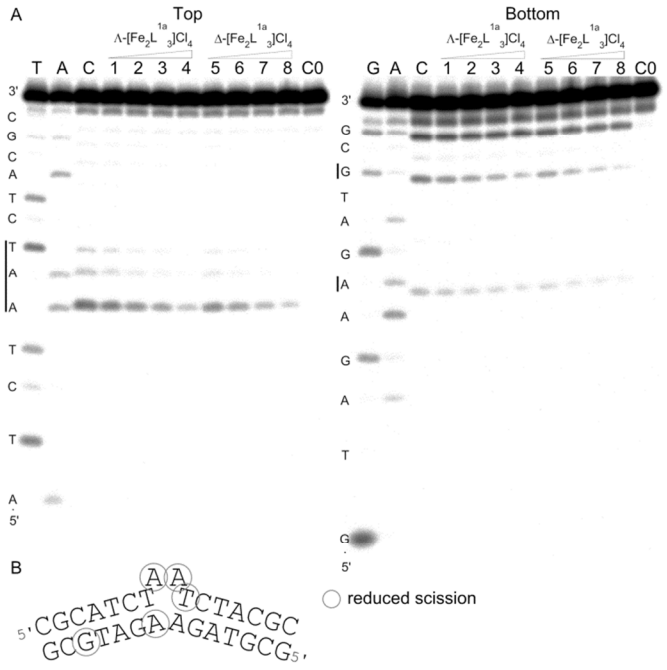

Fig. 3 A. Autoradiograms of DNase I footprint of 5' end labeled top (left) or bottom (right) strand of the 14 bp long DNA duplex containing a two-adenine bulge T-*A2*-T(14) in the presence of different concentrations of Λ-[Fe_2**L**$^{1a}{}_3$]Cl_4 (lanes 1-4) and Δ-[Fe_2**L**$^{1a}{}_3$]Cl_4 (lanes 5-8). Lane C; DNA duplex in the absence of flexicates. Lanes 1-4; DNA duplex mixed with Λ-[Fe_2**L**$^{1a}{}_3$]Cl_4 at 0.25:1, 0.5:1, 0.75:1, and 1:1 (flexicate:DNA duplex) ratios, respectively. Lanes 5-8; DNA duplex mixed with Δ-[Fe_2**L**$^{1a}{}_3$]Cl_4 at 0.25:1, 0.5:1, 0.75:1, and 1:1 (flexicate:DNA duplex) ratios, respectively. Lane C0; DNA duplex in the absence of flexicates and DNase I. Lanes T, A, and G correspond to T, A, and G ladders. The nucleotide sequence of the oligonucleotide is shown on the left side of the gels. B. Sequence of the DNA duplex containing two-adenine bulge showing sites (shown as red circles) protected by Λ- and Δ-[Fe_2**L**$^{1a}{}_3$]Cl_4 from the cleavage by DNase I.

2-Aminopurine fluorescence studies. The fluorescent analogue of adenine, 2-aminopurine (2AP), has been widely used as a probe of small molecule binding to DNA[34,35] or RNA.[36,37] The fluorescence of 2AP is strongly quenched within the structure of double-stranded DNA or RNA, but is enhanced when the base stacking or base pairing is perturbed. Other factors known to affect the fluorescence of 2AP are collisions with other bases and biomolecular interactions.[38,39] In this study we employed the 2AP-labeled T-*A3*-T(14) bulge to directly monitor the binding of Λ- and Δ-[Fe_2**L**$^{1a}{}_3$]Cl_4. The 2AP was incorporated at four different positions either in the loop (Figs. 5B,C) or in the sequence opposite the bulge (Figs. S5A,S5B).

If the 2AP was incorporated in the bulge loop of T-*A3*-T(14) duplex the fluorescence of the 2AP was markedly increased in comparison with its fluorescence when it was incorporated in the fully matched duplex (cf. Figs. 5A-C). The relatively high fluorescence of the 2AP incorporated in the bulge loop is apparently connected with the absence of hydrogen bonding between unpaired 2AP and a complementary base. On the other hand, unpaired purines in the bulges present in the double-helical structure stack into the helix,[40, 41] which can partially quench fluorescence of the unpaired

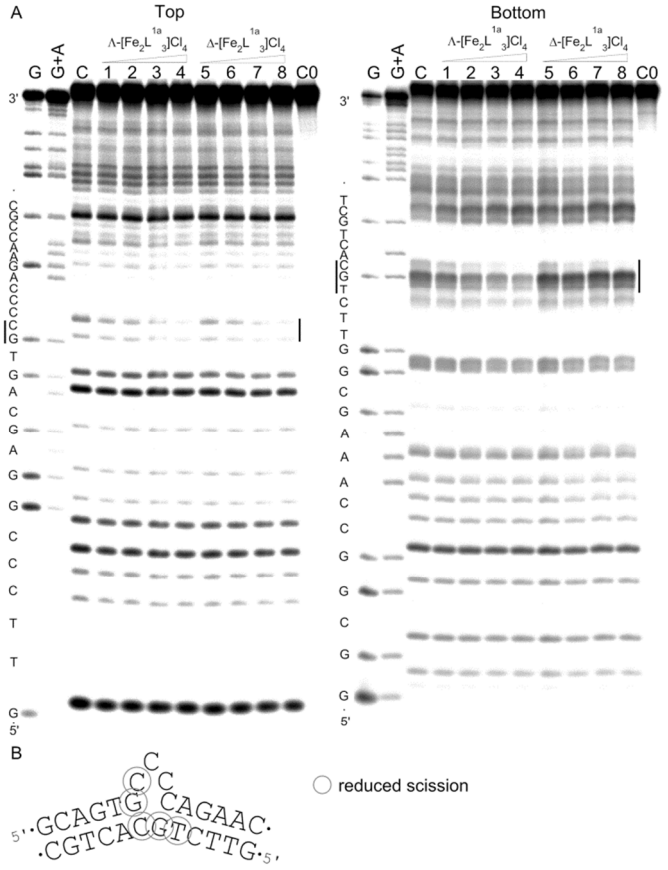

Fig. 4 A. Autoradiograms of DNase I footprint of 5' end labeled top (left) or bottom (right) strand of the 49 bp long DNA duplex containing a three-cytosine bulge G-*C3*-C(49) in the presence of different concentrations of Λ-[Fe_2**L**$^{1a}{}_3$]Cl_4 (lanes 1-4) and Δ-[Fe_2**L**$^{1a}{}_3$]Cl_4 (lanes 5-8). Lane C; DNA duplex in the absence of flexicates. Lanes 1-4; DNA duplex mixed with Λ-[Fe_2**L**$^{1a}{}_3$]Cl_4 at 0.25:1, 0.5:1, 0.75:1, and 1:1 (flexicate:DNA duplex) ratios, respectively. Lanes 5-8; DNA duplex mixed with Δ-[Fe_2**L**$^{1a}{}_3$]Cl_4 at 0.25:1, 0.5:1, 0.75:1, and 1:1 (flexicate:DNA duplex) ratios, respectively. Lane C0; DNA duplex in the absence of flexicates and DNase I. Lanes G, and G+A correspond to Maxam-Gilbert G and G+A ladders. The nucleotide sequence of the oligonucleotide is shown on the left side of the gels. B. Part of the sequence of the DNA duplex containing a three-cytosine bulge showing sites (shown as red circles) protected by Λ- and Δ-[Fe_2**L**$^{1a}{}_3$]Cl_4 from the cleavage by DNase I.

2AP. The observation that the increase of the fluorescence was considerably higher if the AP was incorporated on the 3' side than on the 5' side of the bulge (cf. Figs. 5B,C) can be interpreted to mean that the stacking of the bases on the 3' side of the bulge is perturbed more than on the 5' side.

If the T-*A3*-T(14) bulged duplex was labelled in the sequence opposite the bulge by 2AP, its fluorescence was increased only very slightly in comparison with its fluorescence when the 2AP was incorporated in the fully matched duplex (cf. Figs. S5A,S5B). This slight increase in fluorescence of the 2AP paired with the complementary bases flanking the bulge appears to be due to fluorescence quenching from hydrogen-bonding interactions and base stacking.

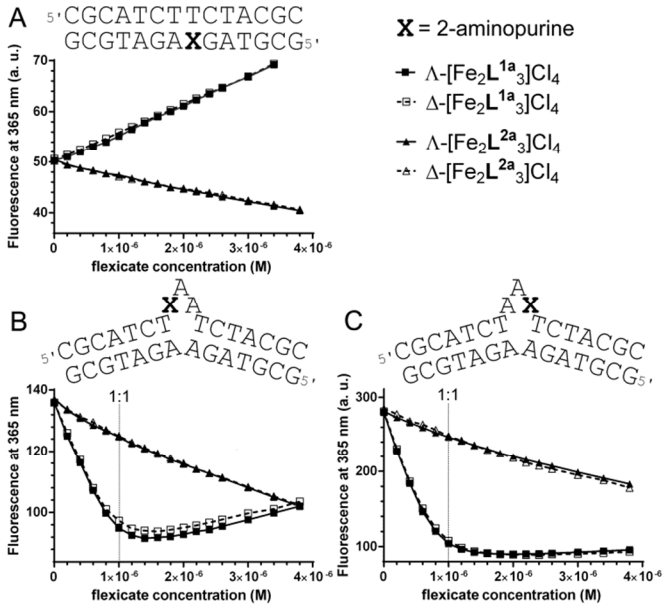

Fig. 5 Fluorescence titrations of the 2AP-labelled fully matched duplex (A) and the T-*A3*-T(14) bulged duplex (1 μM) labelled by 2AP in the bulge loop (B,C) with the enantiomers of $[Fe_2\mathbf{L^{1a}}_3]Cl_4$ and $[Fe_2\mathbf{L^{2a}}_3]Cl_4$ flexicates. The buffer conditions were 10 mM sodium phosphate buffer (pH 7) and 100 mM NaCl.

Titrations of the corresponding fully matched duplex containing 2AP, used as a control, are shown in Fig. 5A. Addition of Λ- and Δ-$[Fe_2\mathbf{L^{1a}}_3]Cl_4$ to the fully matched duplex resulted in a faint, steady increase of the fluorescence intensity. There was no difference between the effects of enantiomers. We demonstrated previously that flexicates based on the $\mathbf{L^{2a}}$ ligand are not very good DNA binders and do not stabilize DNA bulges.[28] Titration of the fully matched duplex with Λ- and Δ-$[Fe_2\mathbf{L^{2a}}_3]Cl_4$ (for its structure, see Fig. 1B) lead to a small linear decrease of the fluorescence intensity (Fig. 5A).

Titrations of the 2AP-labeled T-*A3*-T(14) bulge containing 2AP in the sequence opposite the bulge by Λ- and Δ-$[Fe_2\mathbf{L^{1a}}_3]Cl_4$ resulted only in a small decrease of the fluorescence intensity that culminated at approximately 1:1 flexicate:bulge ratio (Figs. S5B,SC) and then started to moderately increase. The difference between enantiomers was minimal.

Titrations of the 2AP-labeled T-*A3*-T(14) bulge having 2AP incorporated in the bulge loop (Figs. 5B,C) by $[Fe_2\mathbf{L^{1a}}_3]Cl_4$ lead to a marked decrease of the fluorescence intensities up to approximately 1:1 flexicate:bulge ratio. Addition of Λ- and Δ-$[Fe_2\mathbf{L^{2a}}_3]Cl_4$ to the 2AP-labeled T-*A3*-T(14) bulge gave the same results as for the fully matched duplex which is in accordance with the previous results[28] indicating that flexicates based on the $\mathbf{L^{2a}}$ ligand do not recognize DNA bulges. The binding of Λ- and Δ-$[Fe_2\mathbf{L^{1a}}_3]Cl_4$ to the 2AP labelled T-*A3*-T(14) bulge saturates at approximately 1:1 flexicate:bulge ratios, which is consistent with the UV melting studies suggesting a single major binding site for the flexicates on DNA bulges containing two and more unpaired nucleotides. Unexpectedly, the binding of $[Fe_2\mathbf{L^{1a}}_3]Cl_4$ flexicates quenched the fluorescence of 2AP incorporated particularly in the loop of the T-*A3*-T(14) bulge (Figs. 5B,C). It is possible that the binding of the flexicates to the unpaired 2APs in the DNA bulge could quench its fluorescence because the interactions of the flexicates with bases in the bulge loop could restrict their conformational variability. This restriction, presumably contributing to the enhanced thermal stability of the bulged duplexes interacting with the flexicates, could increase the base stacking interactions between the unpaired 2AP and adjacent bases and consequently quench 2AP fluorescence.

The binding of $[Fe_2\mathbf{L^{1a}}_3]Cl_4$ flexicates first quenched the fluorescence of 2AP incorporated in the loop of the T-*A3*-T(14) bulge and at approximately 1:1 flexicate:bulge ratio it started to increase upon further addition of the flexicates (Figs. 5B,C). At present we have no explanation for this observation. We speculate that when the flexicate occupies the major binding site (the bulge) the next molecule interacts with the DNA duplex at a different place, which leads to the fluorescence increase. Fig. 5A demonstrates the interaction of the L1a based flexicates with the 2AP-labelled fully matched duplex which leads to the steady increase of the fluorescence intensity, perhaps due to the perturbed base stacking or base pairing in the presence of the flexicate.

RNA bulges/TAR RNA

Trans-activation response region (TAR) RNA represents an attractive target for the intervention of human imunodeficiency virus type 1 (HIV-1) replication by small molecules. The binding of the viral trans-activator protein, Tat, to the TAR RNA is an essential step in the HIV-1 replication cycle. Therefore, the blockage of Tat-TAR interaction is a potential route for AIDS chemotherapy. Tat binds to TAR RNA at the three-base bulge and interacts with two base pairs above and below in the major groove of TAR RNA.[42] In the present study, we investigated binding of Λ- and Δ-$[Fe_2\mathbf{L^{1a}}_3]Cl_4$ to TAR RNA represented by A-*UCU*-G bulge hairpin (Fig. 6C) and A-*U3*-G RNA duplex (Fig. 6B). The bulged sequences were chosen that exhibit high affinity to the Tat protein.[42] We employed A-*U3*-G TAR RNA duplex since it has been demonstrated that the TAR RNA hairpin can be converted to the TAR RNA duplex (Fig. 6B) without drastically affecting its Tat peptide binding ability.[43]

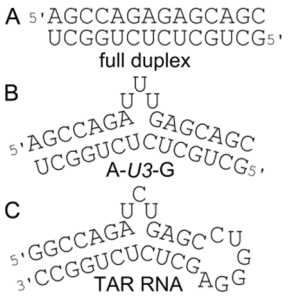

Fig. 6 Sequences of RNA duplexes.

We utilized the measurement of the melting temperature by UV spectroscopy and electrophoretic mobility shift assay to explore binding affinity of Λ- and Δ-$[Fe_2\mathbf{L^{1a}}_3]Cl_4$ to the TAR RNA. The results summarized in Table 5 show that only Δ-$[Fe_2\mathbf{L^{1a}}_3]Cl_4$ had slightly positive impact on the thermal stability of the fully matched RNA duplex (Fig. 6A). The T_m of the A-*U3*-G RNA bulge was increased by 7.2 ˚C and 8.1 ˚C at 1:1 and 2:1 flexicate:bulge ratios, respectively, in the presence of the Λ-enantiomer and by 5.1 ˚C and 5.8 ˚C at 1:1 and 2:1 flexicate:bulge ratios, respectively, in the presence of the Δ-enantiomer. The melting temperature of the TAR RNA was increased by 6.1 ˚C and 7.2 ˚C at 1:1 and 2:1 flexicate:bulge ratios, respectively, in the presence of the Λ-enantiomer and by 4.4 ˚C and 5.6 ˚C at 1:1 and 2:1 flexicate:bulge ratios, respectively, in the presence of the Δ-enantiomer. The $T_m$values of RNA bulges in the presence of Λ- and Δ-$[Fe_2\mathbf{L^{1a}}_3]Cl_4$

were only slightly increased (by 0.7-1.2 ˚C) when the flexicate:bulge ratio was increased from 1:1 to 2:1 which is consistent with a single dominant binding site for the flexicates on these bulges.

Table 5. Thermal stability of the fully matched RNA duplex, the A-*U3*-G RNA bulge and the TAR RNA in the presence of Λ- and Δ-$[Fe_2\mathbf{L^{1a}}_3]Cl_4$.

Compound	ΔT_m (˚C) at 1:1[a]	ΔT_m (˚C) at 2:1[b]
Fully matched RNA duplex (T_m = 62.9 ˚C)		
Λ-$[Fe_2\mathbf{L^{1a}}_3]Cl_4$	-0.6	-0.3
Δ-$[Fe_2\mathbf{L^{1a}}_3]Cl_4$	0.4	1.0
A-*U3*-G (T_m = 46.5 ˚C)		
Λ-$[Fe_2\mathbf{L^{1a}}_3]Cl_4$	7.2	8.1
Δ-$[Fe_2\mathbf{L^{1a}}_3]Cl_4$	5.1	5.8
TAR RNA (T_m = 67.4 ˚C)		
Λ-$[Fe_2\mathbf{L^{1a}}_3]Cl_4$	6.1	7.2
Δ-$[Fe_2\mathbf{L^{1a}}_3]Cl_4$	4.4	5.6

[a] Flexicate:duplex was 1:1. [b] Flexicate:duplex was 2:1.

The autoradiogram of the gel run at 5 ˚C (Fig. S6) shows interactions of the TAR RNA with Λ- and Δ-$[Fe_2\mathbf{L^{1a}}_3]Cl_4$. There is no new slower-migrating band in the gel that would indicate formation of a flexicate-RNA bulge complex in the presence of Λ- and Δ-$[Fe_2\mathbf{L^{1a}}_3]Cl_4$ (Fig. S6, lanes 1-8). Thus, the stability of the flexicate-TAR RNA bulge complexes was not sufficient to withstand migration through a gel.

The Tat-TAR complex has long been considered an attractive target for the discovery of novel antivirals because of its central role in promoting infection by up-regulating HIV transcription. Here, we report that Λ- and Δ-$[Fe_2\mathbf{L^{1a}}_3]Cl_4$ bind to HIV-1 TAR RNA with a promising activity. This finding implies that acting on the TAR RNA by the flexicates may decrease virion production.[44] Research focused on proving sufficient potency and selectivity of these metallohelices to warrant pharmaceutical development is in progress in our laboratory and will be reported in a separate communication.

Conclusions

In summary, our results show that $[Fe_2\mathbf{L^{1a}}_3]Cl_4$ flexicates recognize and stabilize bulged DNA and RNA. Both enantiomers of $[Fe_2\mathbf{L^{1a}}_3]Cl_4$ enhance thermal stability of DNA bulges containing at least one unpaired nucleotide and the stabilizing effect of bound flexicates rises with increasing number of unpaired nucleotides. Our results also demonstrate that the flexicates prefer binding to duplexes containing unpaired pyrimidines in the bulge and pyrimidines flanking the bulge on both 5'-side and 3'-side. Generally, the Λ-enantiomer was more efficient in stabilizing DNA as well as RNA bulges than the Δ-enantiomer. As regards the binding mode of the flexicates to DNA or RNA bulges, the results of our studies indicate that there is only one dominant binding site for the flexicates on the DNA and RNA bulges and that flexicates bind directly to the bulge or in its close proximity. Notably, the $[Fe_2\mathbf{L^{1a}}_3]Cl_4$ flexicates stabilize a DNA bulge containing only one unpaired nucleotide. Nevertheless, the stabilising effect of the flexicates increases with the size of the bulge, but levels off when the bulge contains three and more bases. It seems likely that bulky flexicates based on the the $\mathbf{L^{1a}}$ ligand stick to the bulge from its exterior. However, it cannot be excluded that the $\mathbf{L^{1a}}$ flexicates could also insert into the hollow pocket formed in a three or more nucleotide bulge by unpaired bases. The specific recognition of DNA and RNA bulges by $[Fe_2\mathbf{L^{1a}}_3]Cl_4$ enantiomers could contribute to the biological activity of the flexicates.

Acknowledgements

This work was supported by the Czech Science Foundation (Grant P205/11/0856). The authors also acknowledge that their participation in the EU COST Action CM1105 enabled them to exchange regularly the most recent ideas in the field of platinum anticancer drugs with several European colleagues.

Notes and references

[a]Institute of Biophysics, Academy of Sciences of the Czech Republic, v.v.i., Kralovopolska 135, CZ-61265 Brno, Czech Republic.
[b]Department of Chemistry, University of Warwick, Gibbet Hill Road, Coventry, CV4 7AL, United Kingdom.

†Electronic supplementary information (ESI) available: Fig. S1: Schematic representation of 3D structure of *M*-$[Fe_2(I)_3]^{4+}$; Fig. S2: Melting curves for G-*C2*-G and C-*A2*-C DNA bulges in the presence of Λ- and Δ-$[Fe_2\mathbf{L^{1a}}_3]Cl_4$; Fig S3: Autoradiogram of the gel demonstrating interactions of the flexicates with the T-*A3*-T(14) bulge; Fig. S4: Sequence of the 49-bp long duplex containing a single three-cytosine bulge flanked by guanine and cytosine on the 5'-side and 3'-side, respectively; Fig S5: Fluorescence titrations of the T-A3-T(14) bulged duplex labelled by 2-aminopurine in the sequence opposite the bulge with the flexicates; Fig S6: Autoradiograms of the gels demonstrating interactions of the flexicates with the T-A3-T(14) bulge and TAR RNA. See DOI: 10.1039/b000000x/

1 D. H. Turner, *Curr. Opin. Struct. Biol.*, 1992, **2**, 334-337.
2 M. Chastain and I. Tinoco, *Prog. Nucleic Acid Res. Mol. Biol.*, 1991, **41**, 131–177.
3 V. A. Malkov, I. Biswas, R. D. Camerini-Otero and P. Hsieh, *J. Biol. Chem.*, 1997, **272**, 23811-23817.
4 Y. H. Wang, C. D. Bortner and J. Griffith, *J. Biol. Chem.*, 1993, **268**, 17571-17577.
5 N. Degtyareva, D. Subramanian and J. D. Griffith, *J. Biol. Chem.*, 2001, **276**, 8778-8784.
6 C. Dingwall, I. Ernberg, M. J. Gait, S. M. Green, S. Heaphy, J. Karn, A. D. Lowe, M. Singh, M. A. Skinner and R. Valerio, *Proc. Natl. Acad. Sci. USA*, 1989, **86**, 6925–6929.
7 J. Greenblatt, J. R. Nodwell and S. W. Mason, *Nature*, 1993, **364**, 401–406.
8 D. M. Lilley, *Proc. Natl. Acad. Sci. USA*, 1995, **92**, 7140-7142.
9 Z. Xi, G. S. Hwang, I. H. Goldberg, J. L. Harris, W. T. Pennington, F. S. Fouad, G. Qabaja, J. M. Wright and G. B. Jones, *Chem. Biol.*, 2002, **9**, 925-931.
10 K. Nakatani, S. Sando and I. Saito, *J. Am. Chem. Soc.*, 2000, **122**, 2172-2177.
11 J. A. Smith, J. G. Collins, B. T. Patterson and F. R. Keene, *Dalton Trans.*, 2004, 1277-1283.
12 J. L. Morgan, D. P. Buck, A. G. Turley, J. G. Collins and F. R. Keene, *Inorg. Chim. Acta*, 2006, **359**, 888-898.
13 B. M. Zeglis, J. A. Boland and J. K. Barton, *J. Am. Chem. Soc.*, 2008, **130**, 7530-7531.
14 D. Ma, Y. Lin, Z. Xiao, L. Kappen, I. H. Goldberg, A. E. Kallmerten and G. B. Jones, *Bioorg. Med. Chem.*, 2009, **17**, 2428-2432.

15 I. M. A. del Mundo, K. E. Siters, M. A. Fountain and J. R. Morrow, *Inorg. Chem.*, 2012, **51**, 5444-5457.
16 J. Malina, M. J. Hannon and V. Brabec, *FEBS J.*, 2014, **281**, 987-997.
17 A. Oleksi, A. G. Blanco, R. Boer, I. Usón, J. Aymamí, A. Rodger, M. J. Hannon and M. Coll, *Angew. Chem., Intl. Ed.*, 2006, **45**, 1227-1231.
18 L. Cerasino, M. J. Hannon and E. Sletten, *Inorg. Chem.*, 2007, **46**, 6245-6251.
19 J. Malina, M. J. Hannon and V. Brabec, *Chem. Eur. J.*, 2007, **13**, 3871-3877.
20 H. Yu, X. Wang, M. Fu, J. Ren and X. Qu, *Nucl. Acids. Res.*, 2008, **36**, 5695-5703.
21 I. Meistermann, V. Moreno, M. J. Prieto, E. Moldrheim, E. Sletten, S. Khalid, P. M. Rodger, J. C. Peberdy, C. J. Isaac, A. Rodger and M. J. Hannon, *Proc. Natl. Acad. Sci. USA*, 2002, **99**, 5069-5074.
22 J. Malina, M. J. Hannon and V. Brabec, *Nucleic Acids Res.*, 2008, **36**, 3630-3638.
23 S. E. Howson, L. E. N. Allan, N. P. Chmel, G. J. Clarkson, R. van Gorkum and P. Scott, *Chem. Commun.*, 2009, 1727-1729.
24 S. E. Howson, L. E. N. Allan, N. P. Chmel, G. J. Clarkson, R. J. Deeth, A. D. Faulkner, D. H. Simpson and P. Scott, *Dalton Trans.*, 2011, **40**, 10416-10433.
25 S. E. Howson and P. Scott, *Dalton Trans.*, 2011, **40**, 10268-10277.
26 S. E. Howson, A. Bolhuis, V. Brabec, G. J. Clarkson, J. Malina, A. Rodger and P. Scott, *Nature Chem.*, 2012, **4**, 31-36.
27 A. D. Faulkner, R. A. Kaner, M. A. AbdallahQasem, G. Clarkson, D. J. Fox, P. Gurnani, S. E. Howson, R. M. Phillips, D. I. Roper, D. H. Simpson and P. Scott, *Nature Chem.*, 2014, **6**, 797-803.
28 V. Brabec, S. E. Howson, R. A. Kaner, R. M. Lord, J. Malina, R. M. Phillips, Q. M. A. Abdallah, P. C. McGowan, A. Rodger and P. Scott, *Chem. Sci.*, 2013, **4**, 4407-4416.
29 B. Lustig, I. Baharand and R. L. Jernigan, *Nucleic Acids Res.*, 1998, **26**, 5212-5217.
30 Z. Xi, R. Zhang, Z. Yu, D. Ouyang and R. Huang, *Bioorg. Med. Chem. Lett.*, 2005, **15**, 2673-2677.
31 L. P. Bai, Z. W. Cai, Z. Z. Zhao, K. Nakatani and Z. H. Jiang, *Anal. Bioanal. Chem.*, 2008, **392**, 709-716.
32 M. W. Kalnik, D. G. Norman, M. G. Zagorski, P. F. Swann and D. J. Patel, *Biochemistry*, 1989, **28**, 294-303.
33 M. W. Kalnik, D. G. Norman, B. F. Li, P. F. Swann and D. J. Patel, *J. Biol. Chem.*, 1990, **265**, 636-647.
34 N. Patel, H. Berglund, L. Nilsson, R. Rigler, L. W. McLaughlin and A. Graslund, *Eur. J. Biochem.*, 1992, **203**, 361-366.
35 A. Sielaff, H. Mackay, T. Brown and M. Lee, *Biochem. Biophys. Res. Commun.*, 2008, **369**, 630-634.
36 K. A. Lacourciere, J. T. Stivers and J. P. Marino, *Biochemistry*, 2000, **39**, 5630-5641.
37 T. D. Bradrick and J. P. Marino, *RNA*, 2004, **10**, 1459-1468.
38 B. Holz, S. Klimasauskas, S. Serva and E. Weinhold, *Nucleic Acids Res.*, 1998, **26**, 1076-1083.
39 E. L. Rachofsky, R. Osman and J. B. A. Ross, *Biochemistry*, 2001, **40**, 946-956.
40 L. Joshua-Tor, D. Rabinovich, H. Hope, F. Frolow, E. Appella and J. L. Sussman, *Nature*, 1988, **334**, 82-84.
41 M. A. Rosen, D. Live and D. J. Patel, *Biochemistry*, 1992, **31**, 4004-4014.
42 M. J. Churcher, C. Lamont, F. Hamy, C. Dingwall, S. M. Green, A. D. Lowe, P. J. G. Butler, M. J. Gait and J. Karn, *J. Mol. Biol.*, 1993, **230**, 90-110.
43 J. B.-H. Tok, L. R. Bi and M. Saenz, *Bioorg. Med. Chem. Lett.*, 2005, **15**, 827-831.
44 S. Bannwarth and A. Gatignol, *Curr. HIV Res.*, 2005, **3**, 61-71.